IN-43-CR

86923

Measurement of Surface Physical Properties and Radiation Balance for KUREX-91 Study

P.33

Interim Report for Period
September 15, 1991 - March 15, 1992

NASA Grant NAG5-1762

by

Elizabeth A. Walter-Shea, Blaine L. Blad,
Mark A. Mesarch and Cynthia J. Hays

Department of Agricultural Meteorology
Institute of Agriculture and Natural Resources
University of Nebraska-Lincoln
Lincoln, Nebraska 68583-0728

AgMet Progress Report 92-2
May 1992

ABSTRACT

Biophysical properties and radiation balance components were measured at the Streletskaya Steppe Reserve of the Russian Republic in July 1991 as our contribution to the USA science team investigation during the Kursk Experiment (KUREX-91). Steppe vegetation parameters characterized include: leaf area index (LAI), leaf angle distribution, mean tilt angle, canopy height, leaf spectral properties, leaf water potential, fraction of absorbed photosynthetically active radiation (APAR), and incoming and outgoing shortwave and longwave. Results are presented in Sections 2-4. Section 2 discusses the biophysical parameters. Section 3 discusses the radiation balance estimates. Section 4 discusses sun-view geometry effects on estimating APAR. Results are compared to those of the Konza Prairie in Kansas during the summer of 1989 for the First ISLSCP Field Experiment (FIFE-89).

Incoming and outgoing radiation streams are estimated using bidirectional spectral reflectances and bidirectional thermal emittances. Good agreement between measured and modeled estimates of the radiation balance were obtained. Data used in this study were collected over selected grassland sites on the Streletskaya Steppe Reserve in Russia in July 1991. Agreement between estimated and measured radiation streams are comparable to results obtained during the FIFE study in Kansas in 1987-89.

Instantaneous fractions of absorbed photosynthetically active radiation (APAR) were measured in conjunction with canopy bidirectional-reflected radiation measured at solar zenith angles ranging between 37 and 74° during KUREX-91. APAR values were higher for KUREX-91 than those for FIFE-89 and the amount of APAR of a canopy was a function of solar zenith angle, decreasing as solar zenith angle increased. Differences in absorption are attributed to leaf area index (LAI) and leaf angle distribution and subsequently transmitted radiation interactions. LAI was considerably higher at the Reserve than at the FIFE site. In addition, leaf angle distributions of the Reserve approach a uniform distribution while distributions at the FIFE site more closely approximate erectophile distributions. Reflected PAR components at KUREX-91 and FIFE-89 were similar in magnitude and in their response to solar zenith angle (near constant value). However, transmitted PAR increased with increasing solar zenith angle at KUREX-91 and decreased with increasing solar zenith angle at FIFE-89. Transmitted PAR at FIFE-89 was considerably larger than those at KUREX-91. Spectral vegetative indices derived from canopy bidirectional-reflected radiation are a function of solar and viewing directions indicating that solar and viewing directions must be considered in using remotely-sensed data to derive surface biophysical parameters.

1. INTRODUCTION

The overall unifying objective of the USA KUREX-91 science team component of KUREX-91 is to examine the potential to use remotely sensed data to determine vegetative productivity, to establish relationships between remotely sensed reflected and emitted radiation and productivity, and to understand how various biological factors and various components of the radiation and energy balance may influence or be influenced by the level of productivity. We contributed to the accomplishment of this objective by measuring selected biophysical properties (including leaf optical properties, leaf area index (LAI), and absorbed photosynthetically active radiation) and radiation balance components.

The USA KUREX-91 science team concentrated on taking replicated measures at two steppe sites, one mowed the previous year and one not mowed for many years. Our goals included the characterization of biophysical properties of the steppe vegetation and the characterization of the radiation regime through measurements and from estimates derived from canopy bidirectional reflectance data. Four objectives were identified to meet these goals:

1. Determine dependence of leaf optical properties on leaf water potential of dominant species

2. Characterize the effective leaf area index (LAI) and leaf angle distribution of the steppe vegetation.

3. Characterize the radiation regime of the steppe vegetation through measures of the radiation balance components

4. Examine, develop, and test methods for estimating albedo, APAR and LAI from canopy bidirectional reflectance data.

These objectives relate to the overall USSR KUREX-91 objectives in the following ways:

1. Leaf optical properties, LAI, and leaf angle distribution will provide information on surface characteristics which will support the effort to understand vegetative productivity, APAR and canopy reflectance.

2. LAI will be measured using a nondestructive method and will be available for comparison to destructive measures of LAI.

3. Leaf optical properties measurements, LAI and leaf angle distribution will aid in the determination of phytometric parameters required for hydrological, climatological and vegetative condition dynamics modeling.

4. APAR and LAI measurements will provide information on surface characteristics which will support the effort to understand vegetative productivity and for development of methods for estimating productivity from remotely sensed data.

5. Provide land surface parameters (incoming and reflected [albedo] shortwave and incoming and reflected long wave components, LAI) from which methods of data retrieval from satellite data can be developed.

6. Measurements will provide information required of hydrological and climatological models.

2. BIOPHYSICAL PROPERTIES

2.1 Introduction

Biophysical properties were measured at the Streletskaya Steppe Reserve of the Russian Republic in July 1991 for the Kursk Experiment (KUREX-91). Similar properties were also measured at the Konza Prairie in Kansas during the summer of 1989 for the First ISLSCP Field Experiment (FIFE). These parameters are useful for understanding the radiant energy interaction and outgoing radiation streams needed to interpret remote sensing data.

2.2 Description and Methodology

Biophysical properties were measured in plots located within or near the 50m x 50m PARABOLA area (Figure 2.1) at each of three sites on the steppe identified as Sites 12, 13 and 14. Measurements of LAI, MTA, LAD, canopy height, described in this paper and the measurements of the fraction of instantaneous absorbed photosynthetically active radiation (APAR) (See Sec. 3.2) and canopy temperature (See Sec. 4.2) were measured in five plots encircling the PARABOLA area. Each plot was 9 sq. meter (3m x 3m) with the corners of the plot orientated in the cardinal directions. Two plots of about 15m X 10m in size and separated by about 100m were used for measurements of leaf spectral properties, leaf water potential and stomatal conductance. These two plots were located to the east of the PARABOLA area at Site 12 and to the north at Site 14; no measurements of these properties were made at Site 13.

LAI was measured at least once on the same day that PARABOLA measurements were made. Measurements of LAD, MTA, APAR and stomatal conductance were coordinated with measurements made by the PARABOLA (at designated solar zenith angles). Leaf spectral properties and leaf water potentials were measured independent of sky conditions and were measured throughout the day and also on days when other remote sensing measurements were not made.

LAI, MTA, and LAD were estimated with the LI-COR LAI-2000 Plant Canopy Analyzer. The 270 degree view cap was mounted on the lens and a black tarp was used to shade the area of the canopy the instrument was observing to meet the diffuse requirement of LAI measurements. MTA and LAD measurements did not require the canopy to be shaded (LI-COR, 1991). Three replications were made within each plot during each measurement period and averaged over all measurements for the day.

Heights of the tallest, shortest, medium foliage and inflorescence were measured in each plot. Height were replicated three times; an average foliage and average inflorescence height were calculated. Site 13 was mown so inflorescences were not present. Canopy heights were measured at all Sites early in the experiment and again at Site 12 after a heavy rainfall caused the vegetation to lodge.

Leaf spectral properties and leaf water potential were measured from randomly selected leaves in each of the two plots. Dominant grass species measured were from the genus *Bromus* L. (bromegrass) and *Calamagrostis* Adans. (reedgrass) from both vegetative and reproductive growth stages. The dominant forb species that were measured were *Salvia* L. (sage), *Veratrum* L. (false hellebore) and *Fragaria virginiana* Duchn. (strawberry). Typically two leaves of each grass species and growth stage were measured at each plot on each day of measurement. Forb species were measured only several times during the entire experiment. Hemispherical reflectance and transmittance at near normal incidence were measured with radiometers attached to a LI-COR LI-1800 Integrating sphere. The Nebraska Multiband Leaf Radiometer (NMLR) and the Spectron

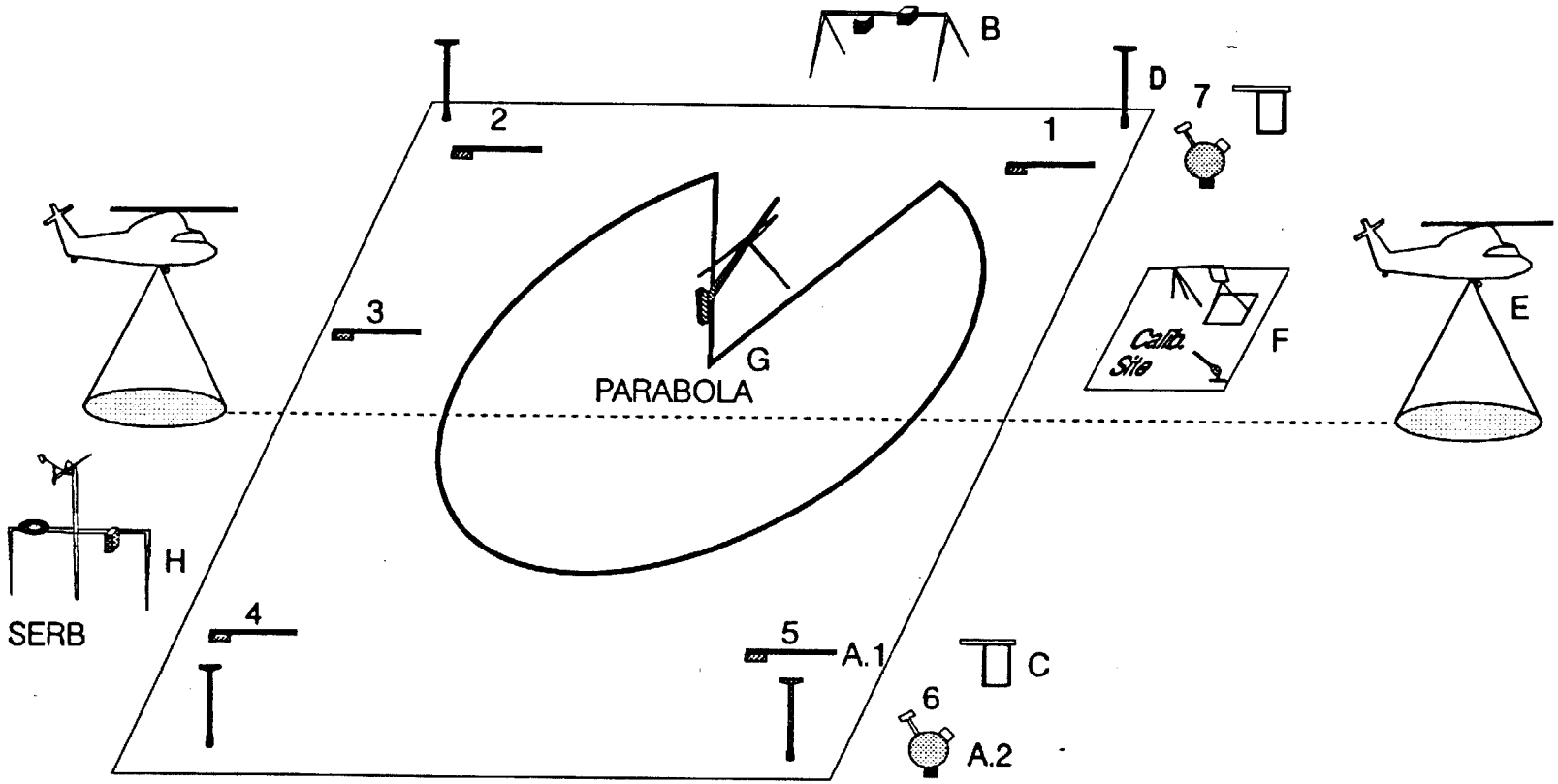

A Numbered Plots:
— A.1 LI-COR LAI-2000 - leaf area index, Schedular - Thermal, LI-COR 191-SA - APAR and IPAR

A.2 NMLR, SE590 & Integrating Sphere - leaf opotics, Scholander Pressure Chamber - leaf water potential

B Surface Radiation Balance:
Inverted Eppley PSP - outgoing shortwave radiation
REBS Net Radiometer - net solar radiation,
Inverted Eppley Pyrgeometer - outgoing longwave radiation
and two Everest Transducers - 0 and 45 degree IR temperature.

C LI-COR 1600 Porometer - Stomatal Conductance

D Gravimetric soil sampling, Soil Impedance Probes

E Helicopter based optical and radar scanners

F Sun Photometer, $BaSO_4$ Panel, Calibration at site 13 only.

G Includes SE590, up & down cameras and pyranometers

H Net solar, reflected solar radiation, diffuse radiation, long wave radiation - up & down, PAR above & below canopy, wind speed & direction, precipitation, air temperature, vapor pressure, soil temperature & heat flow

Figure 2.1 - Physical Layout of KUREX-91 Steppe Study Site Instrumentation

Engineering SE590 were used. The NMLR is a custom-built radiometer which provides spectral coverage in seven similar wavebands as the LANDSAT Thematic Mapper (Mesarch et al., 1991). Pre- and post-calibration of the NMLR indicate that only the first four wavebands were functioning properly; the nominal wavelength limits of these bands are approximately 450-520, 520-600, 630-690 and 760-900 nm. The mean bias error determined from calibration was approximately 0.75 % for wavebands 1-4. The SE590 is a high spectral resolution radiometer which measures over the 400 to 1100 nm wavelength range. The mean bias error determined from calibration for the SE590 was approximately 0.5 % across all the wavebands. Comparison of transmittance from neutral density filters measured with the NMLR and the SE590 (integrated over the wavelengths of the half-band widths of the NMLR wavebands) demonstrate that the NMLR and SE590 are comparable with mean bias errors of -0.15, -1.08, -0.71 and -0.76 for wavebands one through four, respectively.

Leaf water potential was measured with a Scholander-type pressure chamber on the same leaves as had been used for the leaf spectral properties (Stewart and Nielson, 1990). Typically, four additional leaves from surrounding plants of the same species were also measured. Measurements were made predominantly in the mid-morning at the steppe.

Biophysical properties at the Konza Prairie in 1989 were measured similarly as those at the steppe. Only the NMLR radiometer was used to measure leaf spectral properties. Dominant grass species measured on the prairie were *Andropogon gerardii* Vitman (big bluestem), *Panicum virgatum* L. (switchgrass), *Sorghastrum nutans* (L.) Nash (indiangrass) and *Sporobolus asper* (Michx.) Kunth (tall dropseed).

2.3 Results and Discussion

The LAI of KUREX steppe Site 13 was similar to the LAI at the FIFE prairie Site 16 while the LAI at steppe Sites 12 and 14 was considerably larger (Figure 2.2). The large variations in LAI are undetermined. The average LAD and MTA of the KUREX Site 13 and the FIFE Site 16 are similar and represent an erectophile canopy (Figure 2.3). The LAD and MTA for Site 12 and 14 are also similar and represent an uniformly distributed canopy.

Canopy heights were considerably lower at KUREX Site 13 than in Sites 12 and 14 (Table 1).

Table 1 - Canopy height of the Streletskaya Steppe Reserve in 1991.

Site	Date	Height (cm)	
		Foliage	Inflorescence
12	July 10	52.8 ±21.0	133.2 ±6.7
	July 25	47.8 ±17.4	104.4 ±8.8
13	July 10	14.8 ±6.8	N/A
14	July 15	70.6 ±20.9	112.0 ±12.4

Reflectance and transmittance averaged over all grass species and all forb species are typical of spectra of healthy green vegetation (Knipling, 1970) (Figure 2.4). The figure shows close agreement between SE590 and NMLR measured properties. Difference between instruments for the

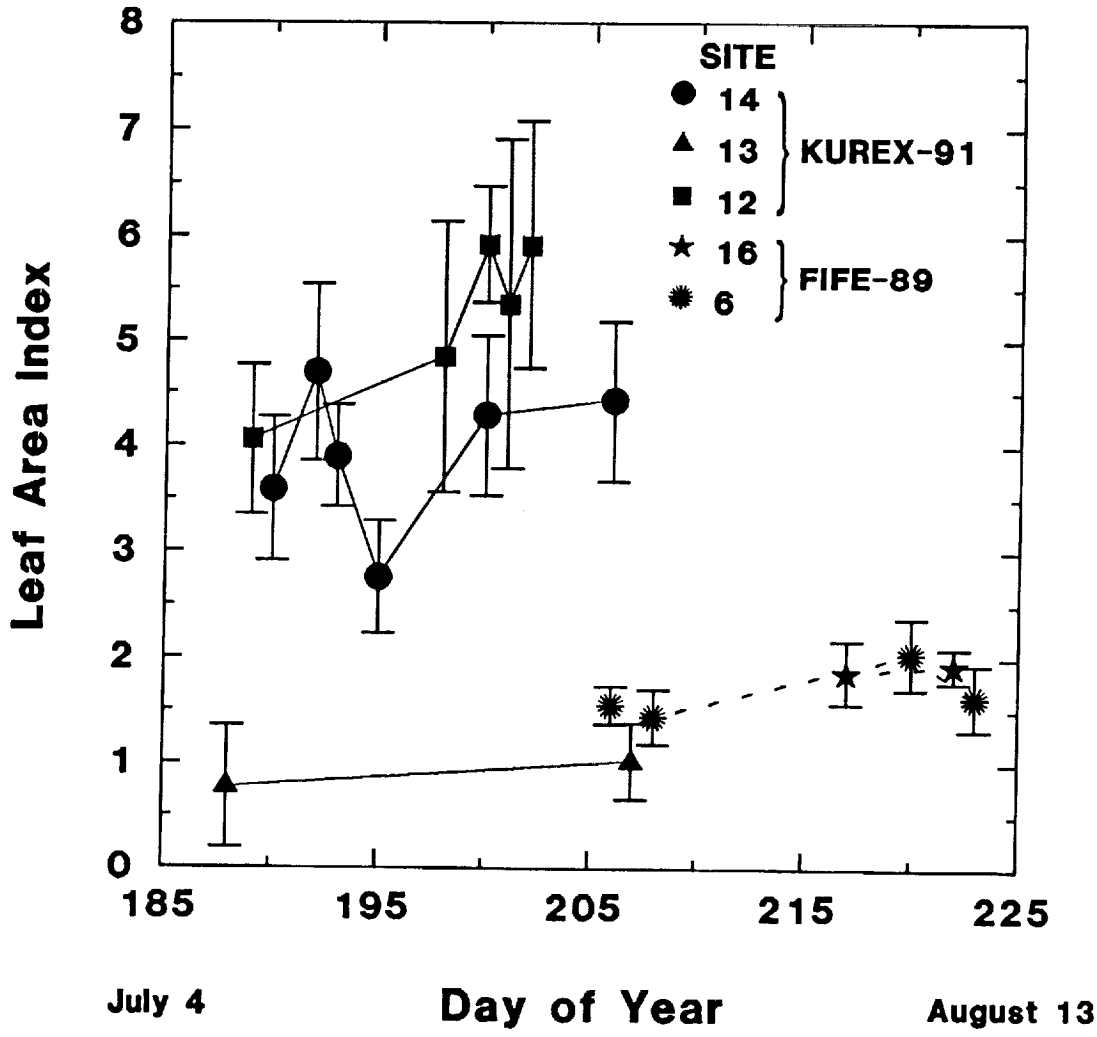

Figure 2.2 - Estimated leaf area index for Sites of the KUREX experiment in 1991 and for Sites of the FIFE experiment in 1989.

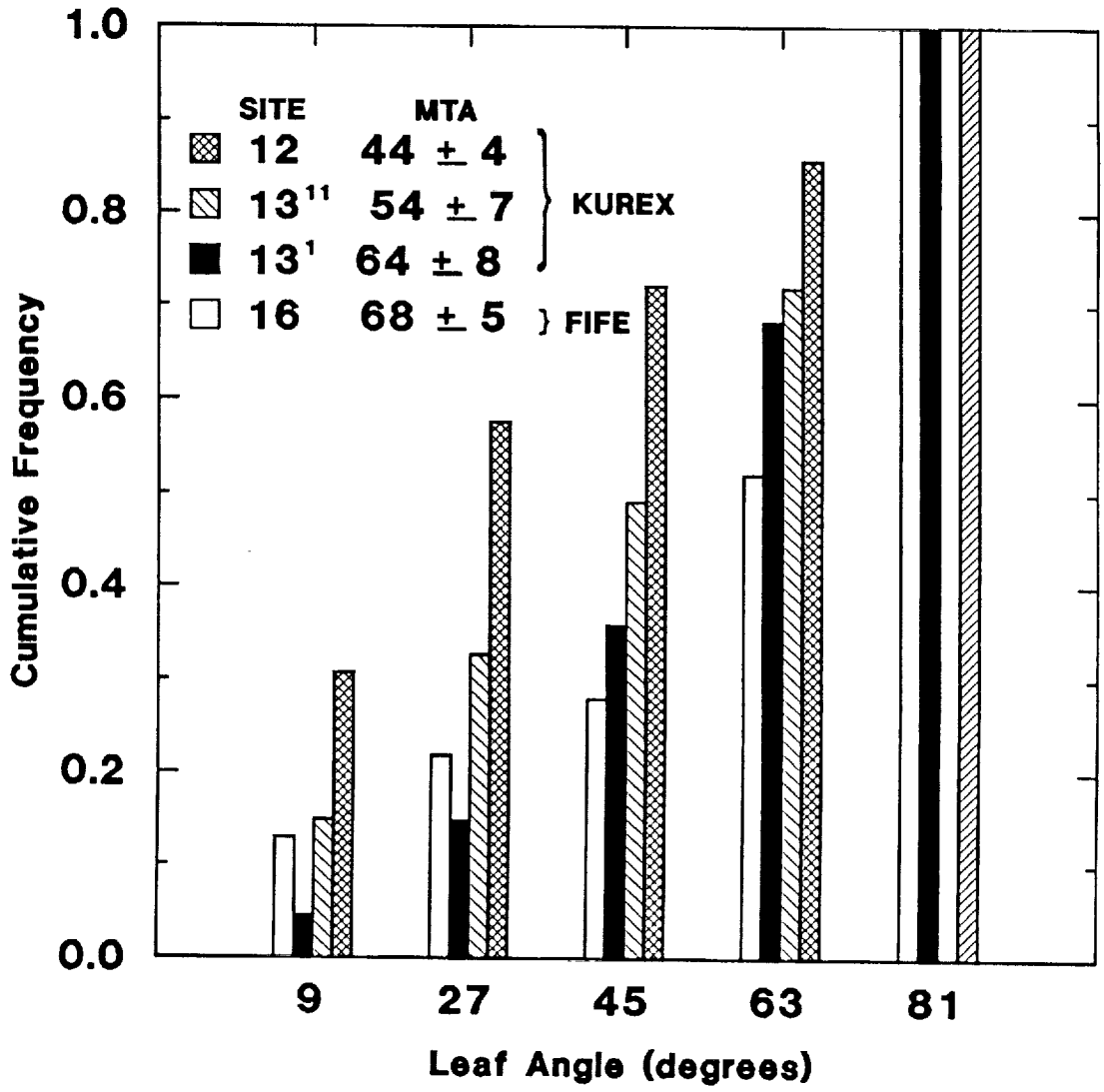

Figure 2.3 - Leaf angle distributions and mean tilt angles for Sites of the KUREX experiment and for the FIFE experiment. [1] KUREX Site 13 measurement taken 7-JUL-91. [11] KUREX Site 13 measurements taken 26-JUL-91

a)

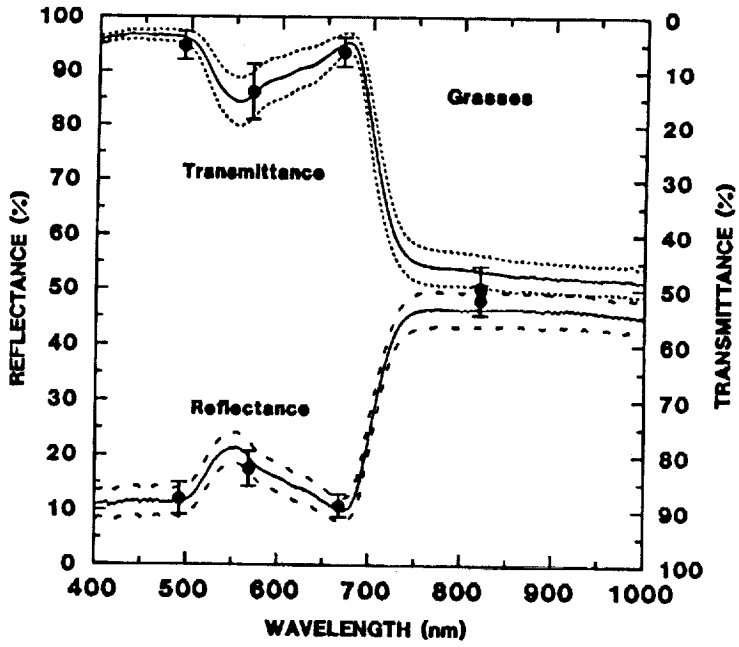

b)

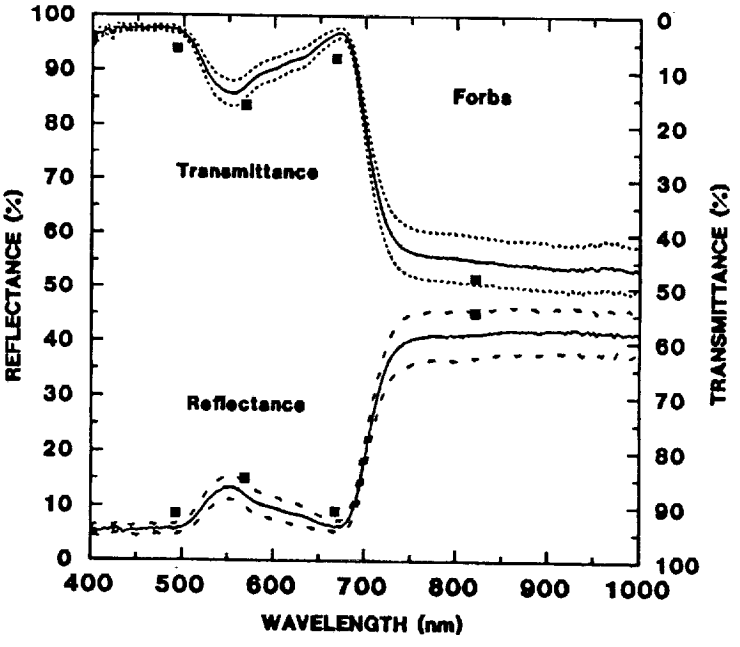

Figure 2.4 - Average leaf reflectance and transmittance measured with the SE590 (solid lines) and the NMLR (points) during the KUREX experiment. Dashed lines and error bars represent one standard deviation from the mean. **a)** Grass leaves and **b)** Forb leaves.

forbs may be influenced most by the limited sampling for measurements with the NMLR (i.e., only two samples of each forbs were measured with the NMLR.)

Using a pooled data set from both radiometers, each species was compared to the other using a Tukey HSD multiple pairwise comparison of the absolute mean differences. For reflectances, the variations within plant group, grasses (0.2-3.7 % reflectance) and forbs (0.8-4.8 % reflectance), can be significant but the variation between plant groups was twice as large (0.4-9.3 % reflectance). Most of the variation is accounted for by the differences in the vegetative growth stage of bromegrass from the other species over several wavebands. For transmittance, the only significant differences occurred between the bromegrass and the reedgrass in several wavebands and between the reedgrass and the false hellebore in the near infrared. Spectral properties were generalized into grass and forb plant groups. Figure 2.5 shows the average and standard deviation for each spectral property for each plant group.

A similar test was conducted on the four grass species measured at the FIFE prairie in 1989. The only significant difference occurred between switchgrass and tall dropseed for transmittance measurements at waveband 4 (821 nm). The range of mean absolute differences for the remaining comparisons was from 0.12 to 2.4 percent reflectance or transmittance.

A comparison was made between each of the species measured at KUREX-91 and FIFE. Bromegrass (vegetative growth stage) reflectance was significantly different from most of the grass species measured at FIFE in wavebands 1, 3 and 4. The other KUREX-91 grasses showed a range of absolute mean differences of 0.2 to 2.7 percent reflectances. The range of differences between the forbs and the FIFE grasses was larger (0.0 to 6.1 percent reflectance), yet did not statistically show significance possibly because of the forbs' small sample size. For transmittances, reedgrass, both vegetative and reproductive growth stages, were significantly different than most of the FIFE grass species for waveband 3 (669 nm). The range of absolute mean differences for the bromegrass compared to the FIFE grasses was 0.2 to 3.2 percent transmittance. The forbs were not statistically different from the FIFE grasses, but differences were large (0.1 to 6.9 % transmittance).

Leaf water potentials ranged from -0.5 to -3.5 MPa. The leaf water potentials measured within hours soon after dawn (21-JULY-91) ranged from -0.5 to -2 MPa. For grasses, the vegetative growth stage plants recovered better than the reproductive growth stage plants. Water potentials measured in the afternoon (on two occasions) were similar to those of the mid-morning hours. However, precipitation had occurred in the previous 24 hours of these days. Leaf water potentials indicate the steppe vegetation was stressed early in the day which was not alleviated during the night or when some moisture was provided. Leaf water potentials from plants at FIFE measured at pre-dawn and throughout the day indicated that these plants tended to recover over night (-0.1 to -0.5 MPa) from stress conditions of -1.0 to -3.0 MPa.

Leaf spectral properties of the KUREX steppe vegetation did not vary with leaf water potentials over the range of -0.5 to -3.5 MPa (Figure 2.6). Similar results were observed at FIFE (Walter-Shea et al., 1992). Differences of bromegrass, vegetative growth stage, and the remaining grass leaves and the forbs are not explained by leaf water potential.

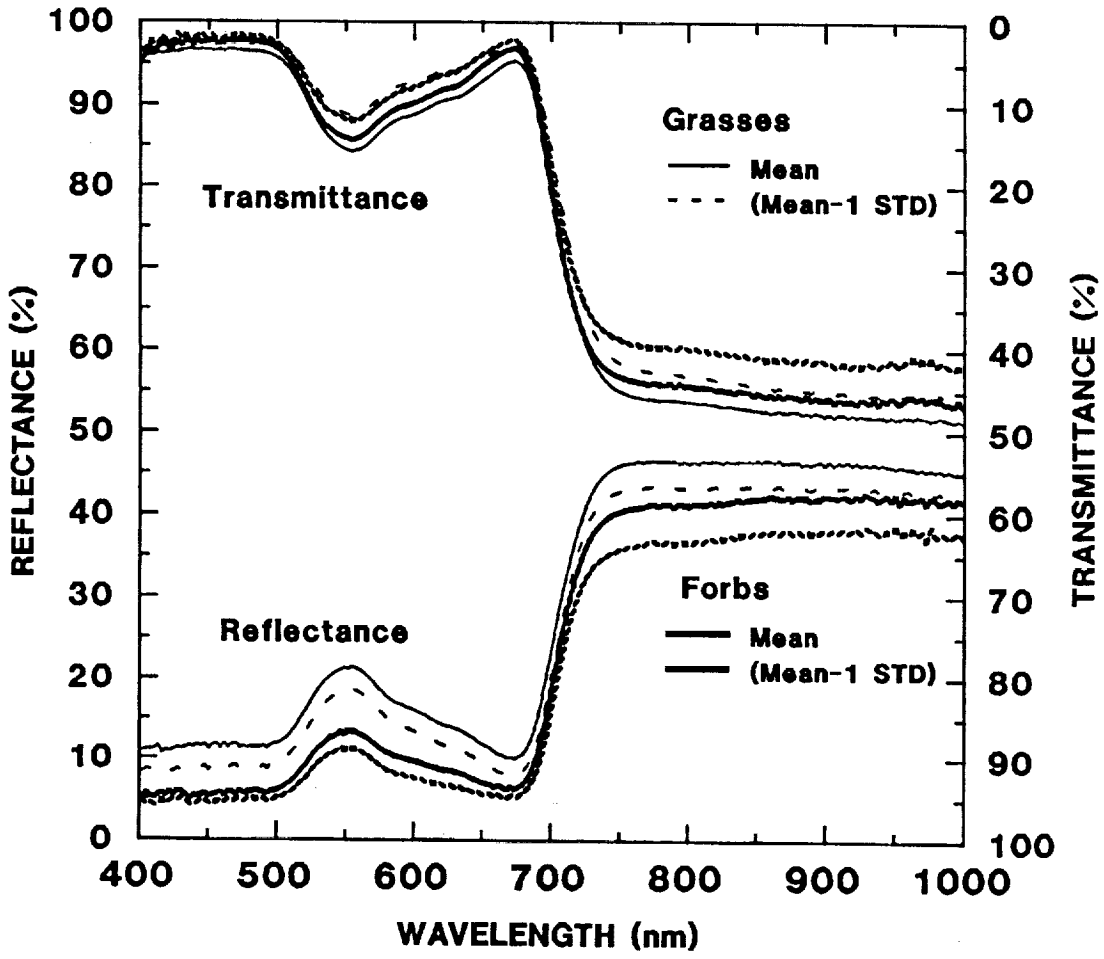

Figure 2.5 - Average leaf spectral properties for both grasses and forbs measured with the SE590 during the KUREX experiment.

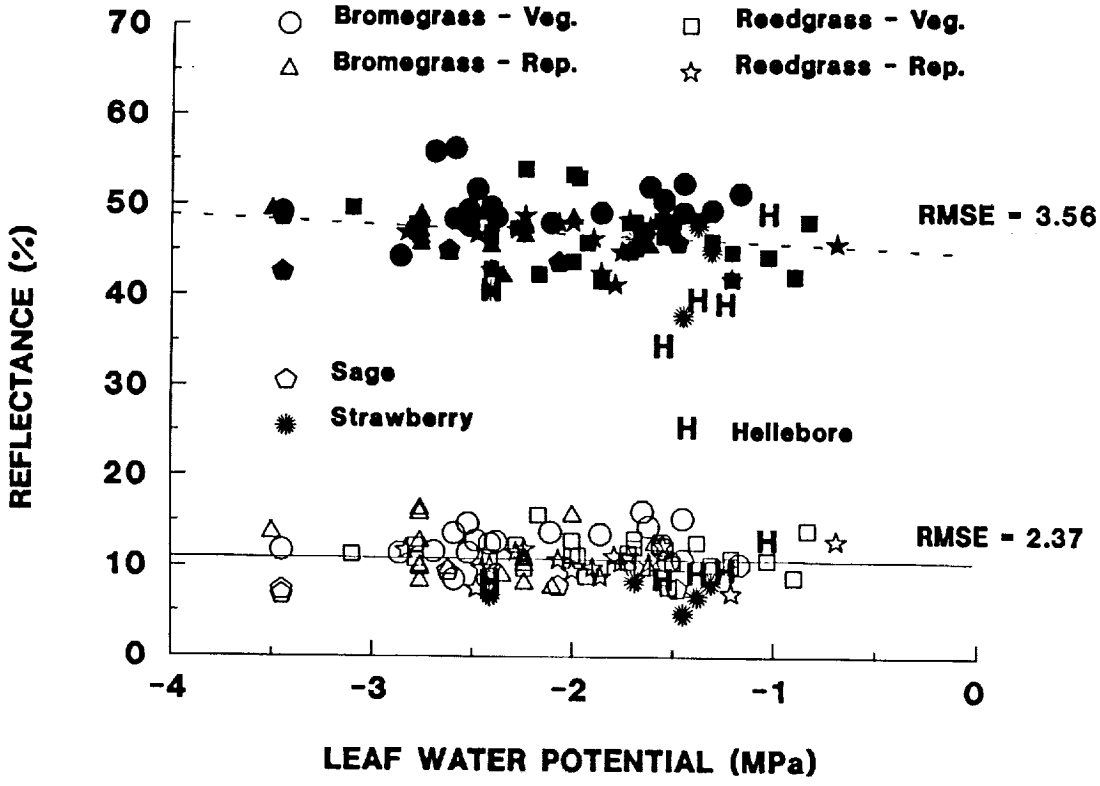

Figure 2.6 - Comparison of leaf water potentials and leaf spectral reflectance measurements made during the KUREX experiment. Leaf spectral measurements made with both the SE590 and NMLR.

3. ESTIMATING REFLECTED AND EMITTED COMPONENTS OF THE RADIATION BALANCE

3.1 Introduction

Net radiation (Rn), the balance of shortwave and longwave radiation streams, is the fundamental quantity of energy available at the earth's surface to drive the processes of photosynthesis, evaporation of water, and heating of the soil and air. Net radiation will vary spatially and temporally. It can be measured at specific locations with net radiometers, but since it is strongly influenced by the surface over which it is measured, it is difficult to extend measurements made at a specific location to other sites, especially if the surfaces are heterogeneous. Remote sensing offers the potential to provide estimates of Rn over different types of surfaces and over areas of various size.

Satellites and other remote sensing instruments do not measure the total hemispherical reflectance or hemispherical emittance directly. Therefore, it is necessary to develop algorithms and techniques to estimate hemispherical reflectances and emittances using spectral data collected by remote sensors. The primary objective of this study is to estimate hemispherical reflectances and hemispherical emittances from grassland surfaces using spectral bidirectional reflectances and bidirectional thermal emittances and to combine these estimates with incoming radiation streams estimated remotely or from readily available weather data to produce reliable estimates of net radiation.

3.2 Materials and Methods

The experiment was conducted on the Streletskaya Steppe Reserve in Russia in July 1991. Data reported here were taken almost exclusively from two grassland sites--a site mowed in 1989 but not in 1990 or 1991 (site 12), and one which had not been mowed for several years (site 14).

Bidirectional reflectance data were obtained with the Goddard PARABOLA instrument (Deering and Leone, 1986) which measures radiation in the 0.650-0.670, 0.810-0.840 and 1.620-1.690 μm waveband regions. For this study, only reflected radiation in the solar principal plane were used. From this principal plane radiance the method of Walthall et al. (1985) was used to simulate directional hemispherical reflected radiation. Incoming shortwave radiation (irradiance) was estimated using reflected radiation obtained over a $BaSO_4$ reference panel using the same method. The SPECTRAL 2 radiative transfer model developed by Bird and Riordan (1984) was used to develop weighting coefficients to extend the spectral data collected by the PARABOLA to the entire solar spectrum. The approach of Starks et al. (1991) was then used to combine the directional-hemispherical reflected radiation and irradiance with weighting coefficients to produce an estimate of the surface albedo.

Bidirectional thermal emittances were determined with the Scheduler Plant Stress Monitor, a hand-held infrared thermometer (IRT). Readings were taken facing the four cardinal compass points in five 2 m x 2 m plots at each site. The IRT was held at an angle of about 45° approximately 1.5 m above the soil surface, and three readings were taken for each direction. The outgoing longwave radiation was calculated using the average of the 12 IRT temperatures taken per plot. Vining and Blad (1990) showed that good estimates of outgoing longwave radiation can be obtained from IRT readings made at a 40° view zenith angle.

Incoming longwave radiation was estimated using the model of Brunt (1932). Several different equations available in the literature for estimating incoming radiation were tested against

measuredincoming longwave radiation in this study and the FIFE study (Starks, 1990). Of all those equations the Brunt model did best here and in the FIFE study.

Each component of the radiation balance was measured using instruments mounted on an A-frame which was moved from site to site and/or from instruments mounted on the SERBS system operated by Dr. Leo Fritschen (1992). For comparison with modeled estimates of incoming and reflected solar radiation measured values of these two radiation streams were obtained from Eppley Precision Spectral Radiometers model PSP operated by Mr. Tom Eck and Dr. Don Deering (1992) in association with PARABOLA measurements. Incoming and outgoing longwave radiation was measured with Eppley Precision Infrared Radiometers (pyrgeometer) model PIR. Net radiation was measured with REBS net radiometers. Instruments were typically mounted 1-1.5 m above the top of the vegetation.

3.3 Results and Discussion

The approach suggested by Starks et al. (1991) was used to estimate the incoming solar radiation flux density. Modeled values are compared with measured values in Figure 3.1. The results show good agreement between measured and modeled values, with a tendency for the model to overestimate the flux density of solar radiation, especially at flux densities below about 500 Wm^{-2}. Statistics for this comparison are shown in Table 3.1.

Table 3.1. Statistics from comparison of incoming shortwave estimations with measured Eppley incoming shortwave longwave values from Deering using the KUREX-91 dataset. N=22.

Algorithm	d	r	r^2	MBE Wm^{-2}	MRE %	RMSE Wm^{-2}	Eu Wm^{-2}	Es Wm^{-2}	x Wm^{-2}	s Wm^{-2}	cv
modelled	0.99	1.00	1.00	25.89	5.95	31.88	10.50	30.10	709.70	182.79	0.26
measured									648.24	205.00	

where
- d = $1 - [\Sigma(E-M)^2/\Sigma(|E-x| + |M-x|)^2]$
- E = estimated value
- M = measured value
- x = mean measured value
- RMSE = $\{[(N^{-1}\Sigma(P-M)^2] + [N^{-1}\Sigma(P-E)^2]\}^{1/2}$
- Es = $(N^{-1}\Sigma(P-M)^2)^{1/2}$
- Eu = $(N^{-1}\Sigma(P-E)^2)^{1/2}$
- P = predicted value from linear regression of estimated and measured values
- MBE = $N^{-1}\Sigma(E-M)$
- MRE = $N^{-1}[\Sigma(E-M)/M)][100]$
- x = $N^{-1}\Sigma E$ or $N^{-1}\Sigma M$
- s = $[(N-1)^{-1}\Sigma(E-x)^2]^{1/2}$ or $[(N-1)^{-1}\Sigma(M-x)^2]^{1/2}$
- cv = s/x

The reflected shortwave radiation stream was estimated with the approach of Starks et al. (1991) using the PARABOLA solar principal plane data. Estimated values are compared with measured values in Figure 3.2. As shown by the statistics given in Table 3.2 there was good agreement between the measured and modeled values but there was a definite trend for the modeled values to be greater than measured values.

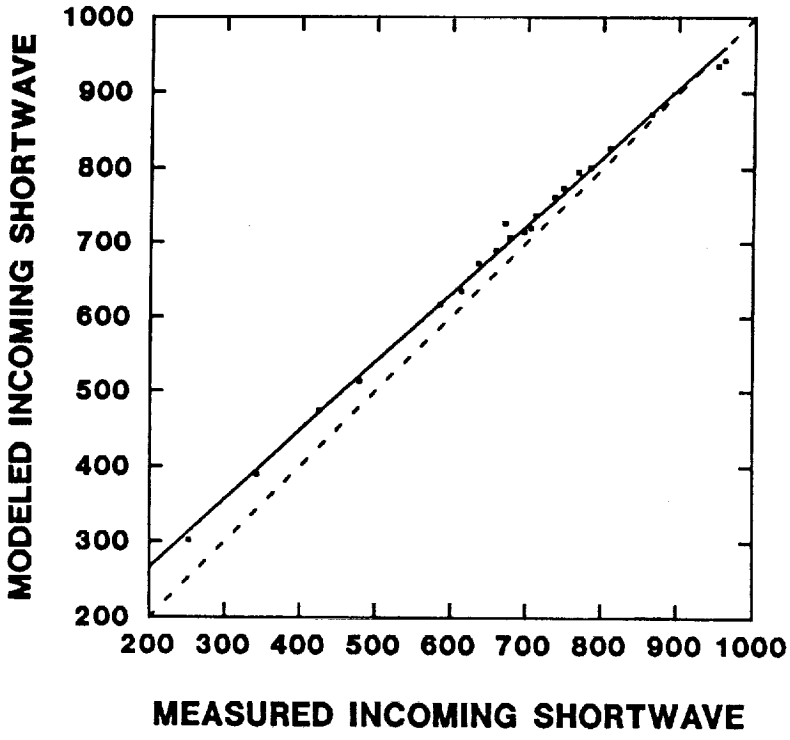

Figure 3.1 Flux densities of incoming solar radiation estimated with the model of [3] Starks et al. (1991) compared with measured values. The dashed line is the 1:1 line.

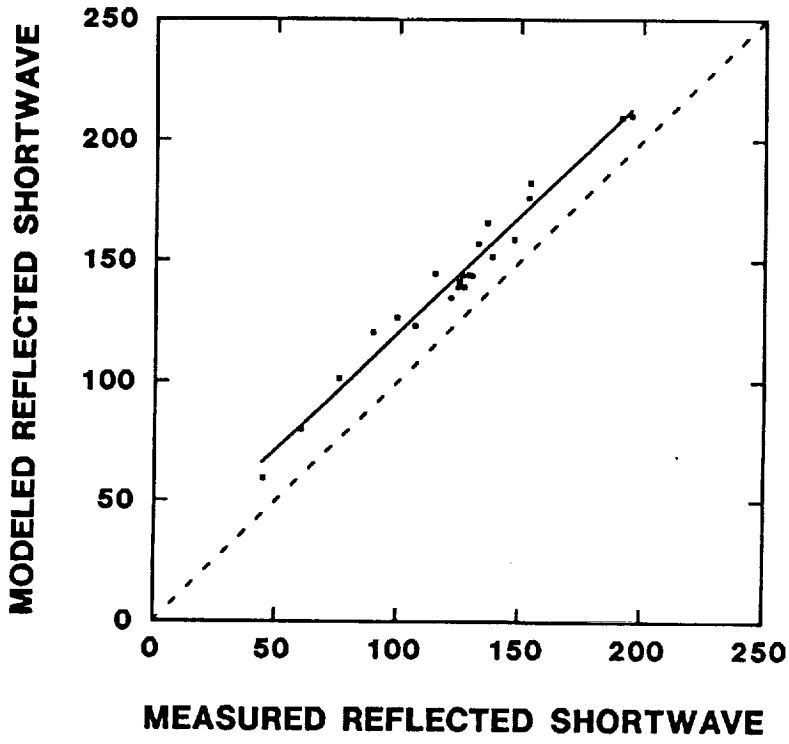

Figure 3.2 Flux densities of reflected solar radiation estimated with the model of [3] Starks et al. (1991) compared with measured values. The dashed line is the 1:1 line.

Table 3.2. **Statistics from comparison of reflected shortwave estimations with measured Eppley reflected shortwave values from Deering using the KUREX-91 dataset. N=22.**

Algorithm	d	r	r^2	MBE Wm^{-2}	MRE %	RMSE Wm^{-2}	Eu Wm^{-2}	Es Wm^{-2}	x Wm^{-2}	s Wm^{-2}	cv
Walthall	0.92	0.98	0.97	19.45	17.71	20.47	6.28	19.48	152.02	36.03	0.24
measured									123.77	36.00	

Data shown in Figures 3.1 and 3.2 were used to calculate the albedo of the surface with the results given in Figure 3.3 and Table 3.3. Modeled values tended to be higher than measured albedo by about 2% with a mean relative error of about 11%. These findings are similar to those reported by Starks et al. (1991) for the data collected during the FIFE study. Possible reasons as to why modeled albedos are higher than measured ones was suggested by Starks et al. (1991) and will not be repeated here.

Table 3.3. **Statistics from comparison of albedo estimations with measured Eppley albedo values from Deering using the KUREX-91 dataset. N=22.**

Algorithm	d	r	r^2	MBE	MRE %	RMSE	Eu	Es	x	s	cv
Walthall	0.78	0.93	0.86	0.022	11.085	0.025	0.010	0.023	0.218	0.026	0.119
measured									0.196	0.022	

The outgoing longwave radiation stream was estimated with the average IRT temperature obtained at the 45° view zenith angle and compared with the measured outgoing longwave radiation stream. Results are shown in Figure 3.4 and Table 3.4. There is very good agreement between the measured and estimated values especially at flux densities between about 375 and 450 Wm^{-2}.

Table 3.4. **Statistics from comparison of outgoing longwave estimations from the average of the Scheduler 45° surface temperature measurements changed to units of Wm^{-2} with measured pyrgeometer outgoing longwave values using the KUREX-91 dataset.**

Algorithm	d	r	r^2	MBE Wm^{-2}	MRE %	RMSE Wm^{-2}	Eu Wm^{-2}	Es Wm^{-2}	x Wm^{-2}	s Wm^{-2}	cv
modelled	0.94	0.93	0.87	4.50	1.02	10.28	8.60	5.63	430.16	24.00	0.06
measured									425.66	18.89	

The incoming longwave radiation stream estimated with the Brunt (1932) equation is compared with the measured stream in Figure 3.5. There is good agreement between measured and modeled values. Statistics for the comparison of estimates of incoming longwave radiation estimated by the Brunt and other models are given in Table 3.5. The Brunt model gave the best estimates of incoming longwave radiation but the modified Deacon and modified Swinbank models also worked quite well.

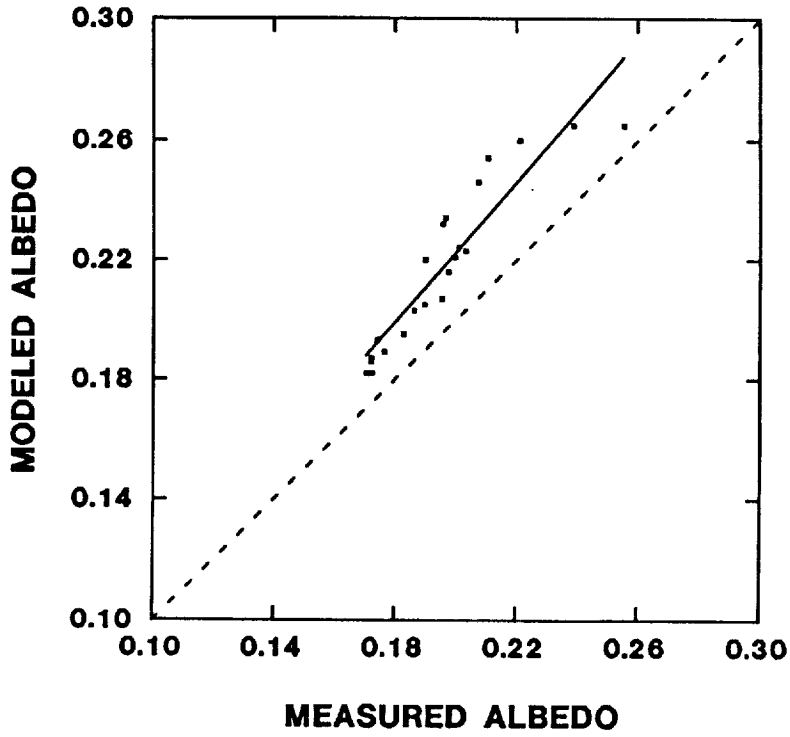

Figure 3.3 Albedo values calculated from incoming and reflected solar flux densities obtained with the [3] Starks et al. (1991) model compared with measured values. The dashed line is the 1:1 line.

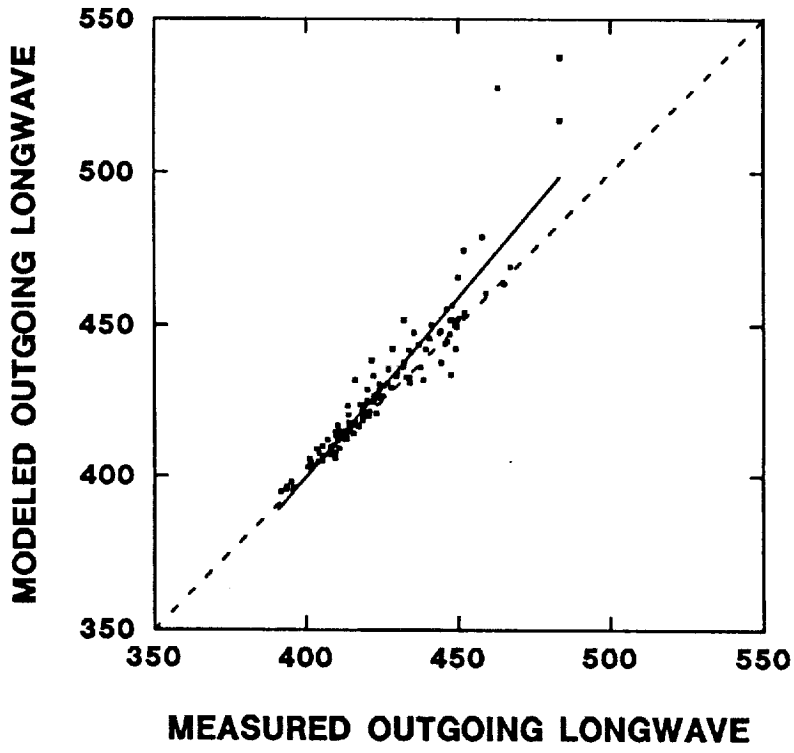

Figure 3.4 Flux densities of outgoing longwave radiation estimated from average canopy temperatures measured with an IRT (Scheduler at a 45° view zenith angle compared with measured values. The dashed line is the 1:1 line.

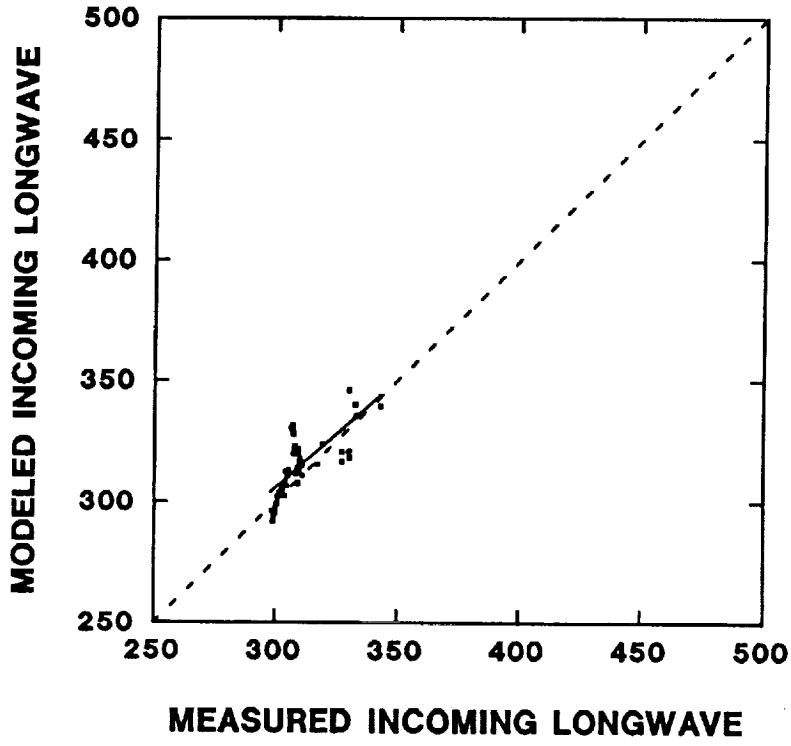

Figure 3.5 Flux densities of incoming longwave radiation estimated with the Brunt equation compared with measured values. The dashed line is the 1:1 line.

Table 3.5. **Statistics from comparison of various incoming longwave estimations with measured pyrgeometer incoming longwave values using the KUREX-91 dataset. N=55.**

Algorithm	d	r	r^2	MBE Wm^{-2}	MRE %	RMSE Wm^{-2}	Eu Wm^{-2}	Es Wm^{-2}	x Wm^{-2}	s Wm^{-2}	cv
Brunt	0.82	0.74	0.55	4.72	1.53	9.26	9.01	2.13	314.97	12.74	0.04
Swinbank	0.33	0.63	0.40	42.28	11.04	41.80	9.02	40.81	350.94	14.35	0.04
mod. Swinbank	0.66	0.63	0.40	10.68	3.46	15.51	11.04	10.90	320.94	14.35	0.04
Deacon	0.35	0.63	0.40	38.83	10.97	38.33	9.02	37.25	347.25	14.26	0.04
mod. Deacon	0.72	0.63	0.40	7.24	2.35	13.23	10.97	7.40	317.49	14.26	0.04
measured									310.26	10.63	0.03

All estimated components of the radiation balance discussed above were combined to give an estimate of Rn. The estimated Rn was then compared with Rn measured on the A-frame (Figure 3.6). There is excellent agreement between estimated and modeled values as shown by the comparison statistics given in Table 3.6. It is interesting to note that the Rn estimated using the procedures described above agreed better with the measured Rn than when the radiation balance was calculated using measured components of each incoming and outgoing radiation stream (Table 3.6). The reason for the better agreement of the estimated Rn and the component calculated Rn with measured Rn is not certain, but is probably related to the fact that most of the measured components were made at different locations than the place where the Rn was measured. In the FIFE study the calculation of Rn using measured components agreed better with measured Rn than did the Rn estimated using the models similar to those in this study. There was better agreement between measured and estimated Rn in the KUREX-91 study than was found in the FIFE study.

Table 3.6. **Statistics from comparison of Rn from estimated components (reflected shortwave-Walthall model, incoming longwave -Brunt model, outgoing longwave average of 45° Scheduler), measured components (incoming and reflected shortwave - Deering data, incoming longwave Fritschen data, outgoing longwave A-frame data), measured by the REBS net radiometer on the A-frame.**

Method	d	r	r^2	MBE Wm^{-2}	MRE %	RMSE Wm^{-2}	Eu Wm^{-2}	Es Wm^{-2}	x Wm^{-2}	s Wm^{-2}	cv
Measured components	0.98	0.97	0.95	4.59	0.63	26.54	25.81	6.16	508.30	91.68	0.18
Estimated components	0.99	0.99	0.98	3.82	0.92	23.12	19.37	12.64	507.52	72.82	0.14
measured									503.71	77.08	0.15

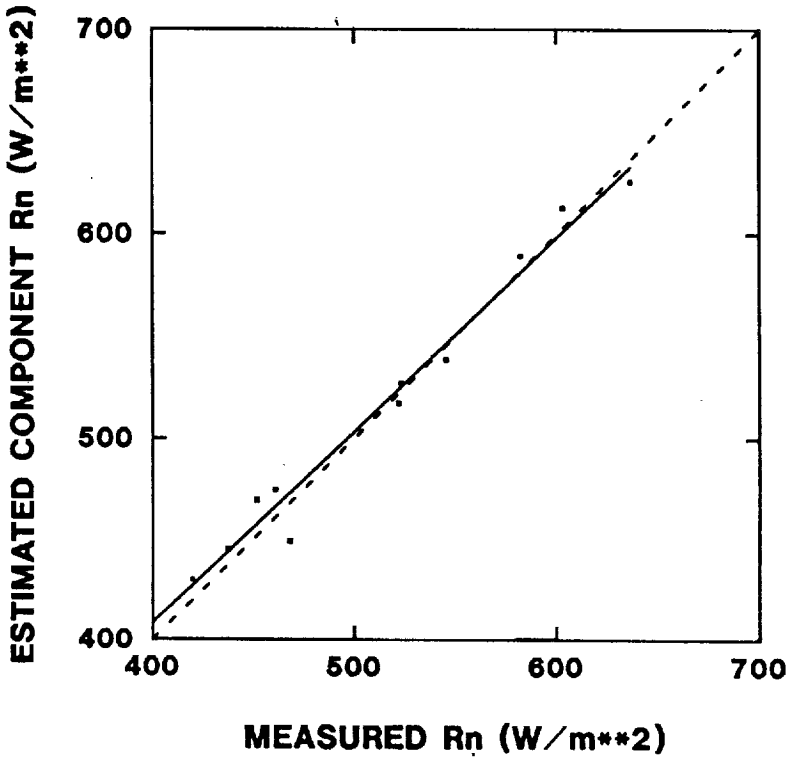

Figure 3.6 Flux densities of net radiation estimated from the radiation balance components in figures 2-6, compared with Rn measured with the REBS net radiometer on the A-frame. The dashed line is the 1:1 line.

4. ABSORBED PHOTOSYNTHETICALLY ACTIVE RADIATION AND SUN-VIEW GEOMETRY EFFECTS ON APAR ESTIMATES

4.1 Introduction

Photosynthetically active radiation (PAR) absorbed by vegetation is an essential parameter in understanding vegetative photosynthetic capacity and surface conductance used in regional and global carbon cycle studies. The amount of radiant energy attenuated in a canopy is a function of leaf optical properties and canopy geometry, in particular leaf area index, leaf angle distribution and gap fraction. The PAR fraction intercepted and absorbed is a function of solar zenith angle (Hipps et al., 1983). Remote sensing can potentially provide data from which the fraction of intercepted and absorbed PAR can be estimated using ratios of reflected visible and near-infrared (NIR) radiant energy known as spectral vegetative indices (SVIs). Two common SVIs are the simple ratio (SR=NIR/visible) and the normalized difference vegetative index (NDVI=[(NIR-visible)/(NIR+visible)]. Asrar et al. (1984) demonstrated that NDVI and absorbed PAR are functions of LAI. The value of the SVIs varies as a function of solar and viewing directions (Deering and Middleton, 1990; Cornell 1991). Sellers (1985) demonstrated through the use of a simple radiative transfer model that SVI dependence on solar zenith angle was a function of canopy architecture and may diminish with large LAI.

The objective of this paper is to characterize instantaneous fractions of absorbed PAR (APAR) so that relationships between APAR and remotely-sensed-derived bidirectional SVIs can be understood.

4.2 Methodology

Incoming ($K\downarrow_{par}$), reflected ($K\uparrow_{par}$) and transmitted ($K\downarrow_{tpar}$) PAR received on one meter in length horizontal surfaces above and within the steppe vegetation were measured at five representative plots at KUREX-91 Sites 12 and 14 with a LI-COR LI-191SA Line Quantum Sensor. From these measurements, instantaneous fractions of reflected, transmitted, intercepted and absorbed PAR (RPAR, TPAR,IPAR and APAR, respectively) were calculated. Measurements were coordinated with PARABOLA canopy bidirectional reflected radiation measurements completed over solar zenith angles ranging from 37 to 74°. Also a LI-COR LI-190S Quantum Sensor was mounted for point measurements of incoming PAR at Site 14 and two sensors were mounted within the canopies for measurements of transmitted PAR (Fritschen, 1992). These measurements yielded near-continuous measurements of incoming and transmitted PAR from which TPAR and IPAR were calculated.

Fractions of reflected and transmitted PAR are simply the ratios of reflected and transmitted PAR to total incoming PAR, i.e., $K\uparrow_{par}/K\downarrow_{par}$ and $K\downarrow_{tpar}/K\downarrow_{par}$, respectively. Instantaneous fractions of intercepted and absorbed PAR were calculated as:

$$IPAR = 1 - TPAR \tag{4.1}$$

$$APAR = IPAR * (1 - RPAR) \tag{4.2}$$

The fraction of PAR transmitted through the canopy which is direct beam (T_{beam}) was estimated from the expression based on Beer-Bourger's law (assuming azimuthal symmetry):

$$T_{beam} = \frac{\exp[(-G)(LAI)/\cos\theta_s)}{TPAR} \tag{4.3}$$

where G is the extinction coefficient (a function of leaf angle distribution), LAI is the leaf area index for the canopy and θ_s is the solar zenith angle. The remaining fraction is attributed to be the fraction of PAR penetrating the canopy which is diffuse radiation.

The Normalized Difference Vegetation Index (NDVI) and Simple Ratio (SR) were computed using reflected radiances collected from the PARABOLA over vegetation representative of the vegetation from which IPAR and APAR were measured (Eck and Deering, 1992). Due to weather conditions during KUREX-91, a complete diurnal range of solar zenith angles was not represented.

4.3 Results and Discussion

Instantaneous fractions of absorbed PAR were higher at small solar zenith angles than at large solar zenith angles (values of 0.95-0.85 vs 0.75) (Figure 4.1). Instantaneous fractions of reflected and transmitted PAR were low and increased as solar zenith angle increased (Figure 4.2) and thus resulted in decreasing values of APAR. The absolute changes in RPAR and TPAR over the range of PARABOLA measurements were approximately 15 and 10%. Point quantum sensors indicated that TPAR continued to increase beyond those measured with the line quantum sensor as solar zenith angle increased (Figure 4.2). (Note: continuous measurements of TPAR agree well with the discrete measurements with the line quantum sensor).

Fraction of transmitted direct beam radiation was calculated from Eq. 3 using values of G equal to 0.5 (representing a canopy with a spherical leaf angle distribution) and LAI equal to 3.9 and 5.6 (representing Sites 12 and 14, respectively) (See Section 2.3). At solar zenith angles of 45° or less it is estimated that approximately 75% or more of the PAR transmitted through the canopy is direct beam and at solar zenith angles of 65-70° all direct beam is intercepted by the canopy (Figure 4.3). Thus, the majority of PAR transmitted at large solar zenith angles must be diffuse radiation. In contrast, data collected at the First ISLSCP Field Experiment in 1989 (FIFE-89) indicated APAR values considerably lower than those at KUREX-91 and exhibiting a tendency for APAR to increase as solar zenith angle increased over solar zenith angles of 20-50° (Figure 4.4). Reflected fraction of PAR changed little as a function of solar zenith angle but TPAR decreased with increasing solar zenith angle, a contrast to TPAR measured at KUREX-91 (Figure 4.5). More radiation penetrated the vegetation to the soil surface as solar zenith angle increased (as direct beam theory predicted). Direct beam dominated at these angles for a canopy with vertical leaves and low LAI of 1.5-2.0 (Figure 4.3). Similar fractional components were noted in a wheat canopy with a LAI of 1.4 (Fuchs et al., 1984).

SVIs varied with solar and view zenith angles (Figure 4.6). SVIs were symmetrical about nadir for Site 14 while those for Site 12 were asymmetrical about nadir. Values of SR derived from forward, backscatter and nadir reflected radiances varied in value from approximately 4 to 7 for Site 14 data while the SR values for Site 12 varied from 3 to 5. NDVI values varied in a similar manner.

The general magnitude of SVIs agree with LAI and APAR data in that Site 14 has higher values associated with higher LAI and APAR values than Site 12 (Compare Figures 4.1 and 4.6). Researchers have suggested that SVIs should be linearly related to APAR. Results from FIFE-89 showed that this varied according to view zenith angle, being linear functions for nadir- and forward scatter-derived SVIs but not for backscatter-derived SVIs (Walter-Shea et al., 1992). A similar investigation with KUREX-91 data reveals similar trends.

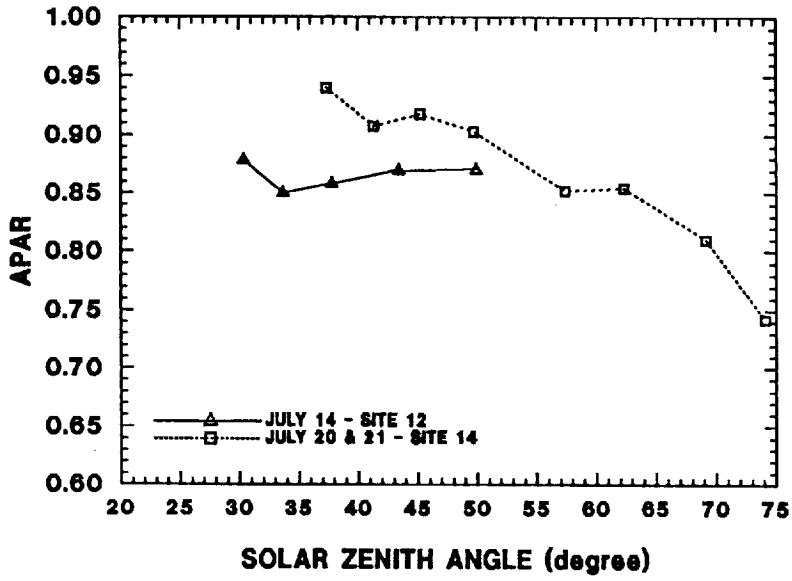

Figure 4.1 Instantaneous fractions of absorbed photosynthetically active radiation (APAR) as a function of solar zenith angle at KUREX-91 Site 12 (July 14) and Site 14 (July 20 and 21).

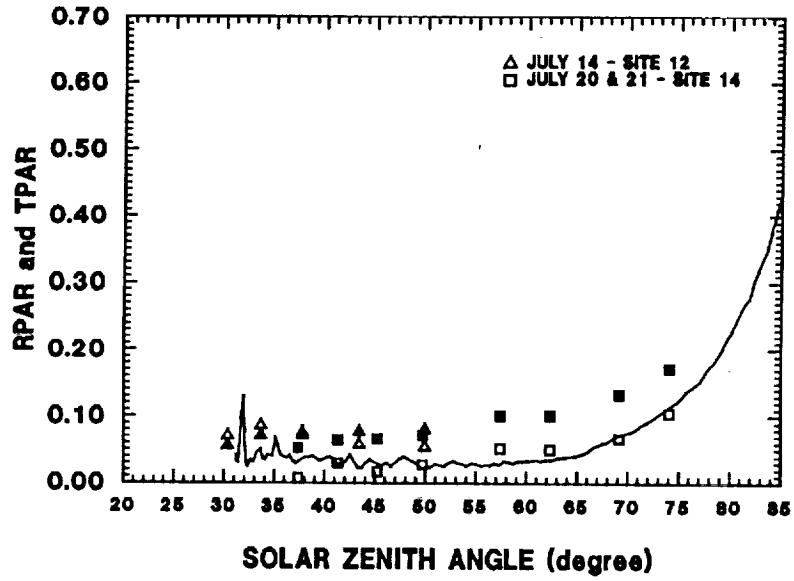

Figure 4.2 Instantaneous fractions of reflected and transmitted photosynthetically active radiation (RPAR and TPAR) at KUREX-91 Site 12 (July 14) and Site 14 (July 20 and 21). RPAR values are represented with filled symbols; TPAR values are represented with open symbols.

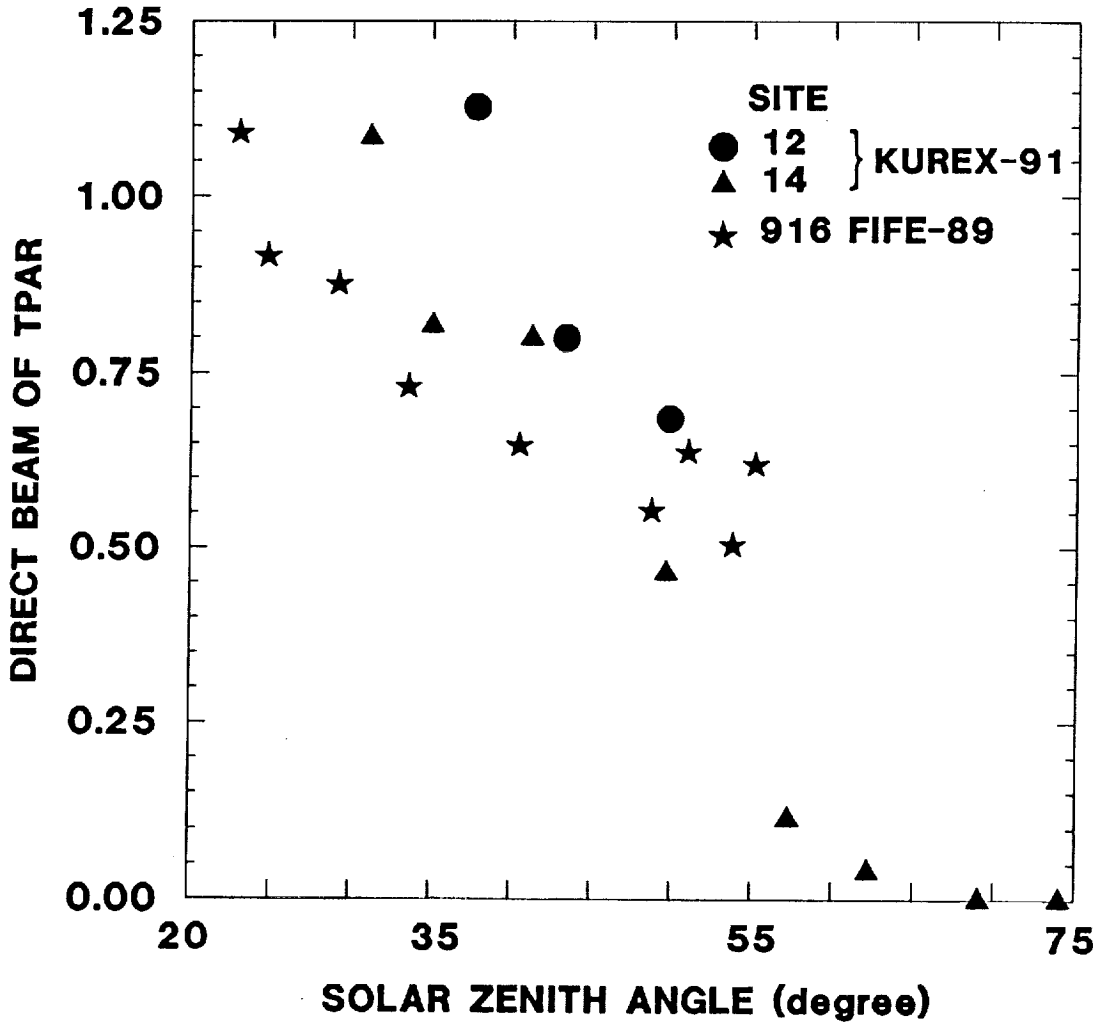

Figure 4.3 - Direct beam fraction of transmitted photosynthetically active radiation (TPAR) estimated using Eq. 3 at KUREX-91 Site 12 (July 14), Site 14 (July 20 and 21) and FIFE-89 Site 916 (July 28, August 4 and August 8).

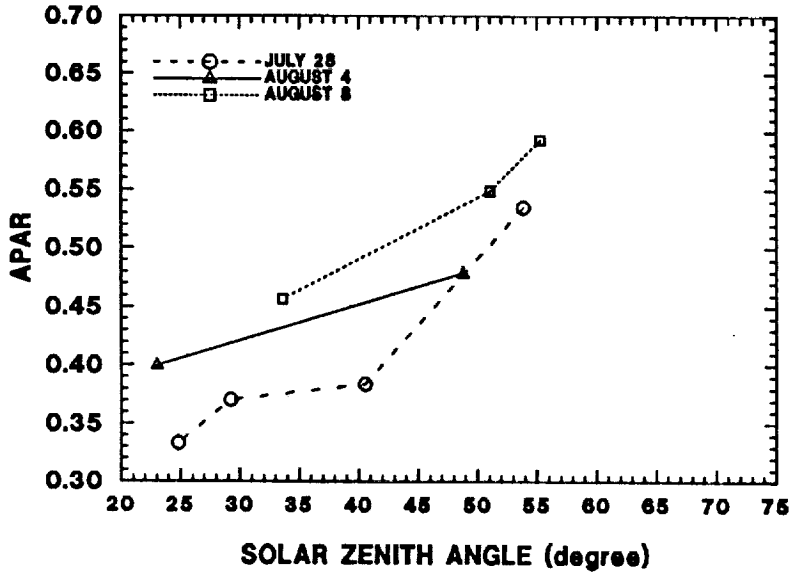

Figure 4.4 Instantaneous fractions of absorbed photosynthetically active radiation (APAR) as a function of solar zenith angle at FIFE-89 Site 916 (July 28, August 4 and August 8).

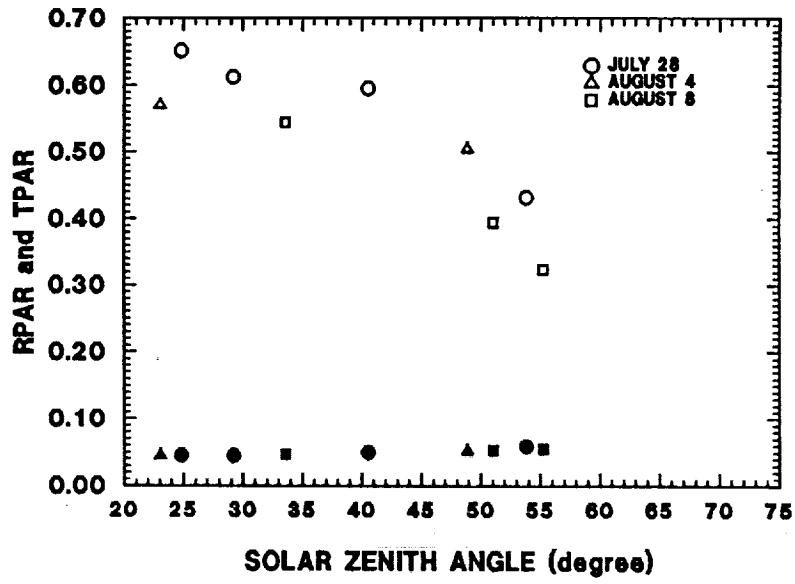

Figure 4.5 Instantaneous fractions of reflected and transmitted photosynthetically active radiation (RPAR and TPAR) at FIFE-89 Site 916 (July 28, August 4 and August 8). RPAR values are represented with filled symbols; TPAR values are represented with open symbols.

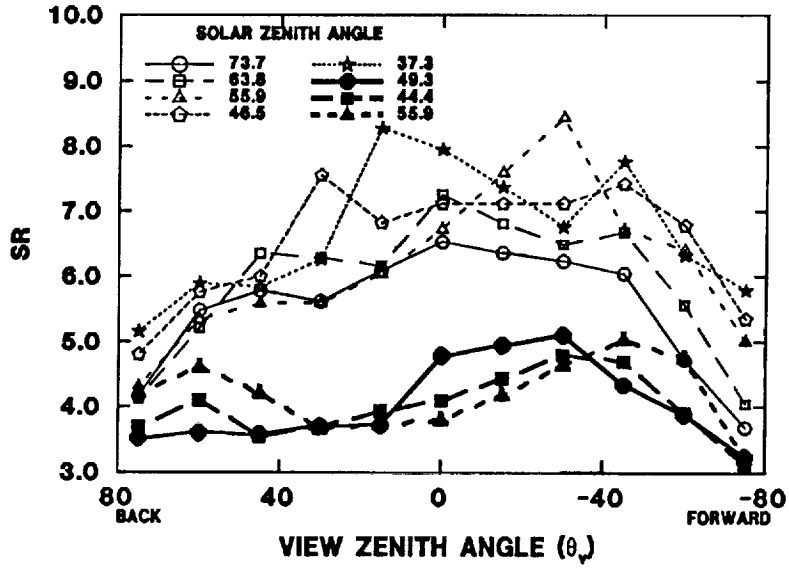

Figure 4.6 Simple ration (SR=near-infrared/visible) derived from PARABOLA radiances as a function of solar and view zenith angles at KUREX-91 Site 12 (July 14) (filled symbols) and Site 14 (July 20 and 21) (open symbols).

5. CONCLUSIONS

Data collected during KUREX-91 provides information useful in comparing canopy bidirectional reflectances measured at the Streletskaya Steppe and the Konza Prairie. Generally, the steppe was characterized by high LAIs and an uniform LAD, while the prairie was characterized by low LAIs and an erectophile canopy. The magnitude of the leaf spectral properties and the relationship between spectral properties and leaf water potential, ranging from -0.5 to -3.5 MPa observed at the KUREX and FIFE Sites, are comparable.

The algorithms and procedures developed and/or tested in FIFE to estimate Rn and its component parts worked very well for estimating the flux densities of incoming and outgoing radiation and net radiation in the KUREX-91 study. In fact, they actually produced better estimates when compared to measured values than was observed for the FIFE data. The results of these studies suggest that Rn can be reliably estimated using remote sensing techniques.

Radiative transfer through the grassland vegetation of the KUREX-91 and FIFE-89 sites differed resulting in differences in absorbed photosynthetically active radiation (APAR), indicative of differing productivities. Remote sensing offers a means of determining the productivity of vegetative surfaces but results indicate further study is warranted to identify the effects of solar and view angles on spectral vegetation indices and estimates of absorbed photosynthetically active radiation. Results at FIFE and KUREX-91 indicate spectral vegetation indices (SVIs) derived from reflected radiation in the backscatter direction may provide reliable estimates of daily APAR since SVI is near constant regardless of solar zenith angle.

6. REFERENCES

G. Asrar, M. Fuchs, E. T. Kanemasu and J.L. Hatfield, "Estimating absorbed photosynthetic radiation and leaf area index from spectral reflectance in wheat," *Agronomy Journal*, vol. 76, pp. 300-306, 1984.

R. Bird and C. Riordan, Simple solar spectral model for direct and diffuse irradiance on horizontal and tilted planes at the earth's surface for cloudless atmospheres. Solar Energy Research Institute, Golden, CO, 1984, 1984.

D. Brunt, "Notes on radiation in the atmosphere 1," *Quart. J. Roy. Meteorol. Soc.*, Vol. 58, pp. 389-418, 1932.

D. Cornell, "Sun-view-target geometry effects on spectrally-derived vegetative index estimates of absorbed radiation and leaf area", M.S. Thesis, University of Nebraska, pp. 132, 1991.

D. W. Deering and P. Leone, "A sphere-scanning radiometer for rapid directional measurements of sky and ground radiance," *Remote Sensing Environment*, Vol. 10, pp. 1-24, 1986.

D.W. Deering and V.V. Kozoderov, "KUREX-91: A U.S.S.R./U.S. study for global climate processes in steppe vegetation," in *Proceedings of the International Geoscience and Remote Sensing Symposium*, Houston, Texas, May 26-29, 1992.

D. W. Deering and E. M. Middleton, "Spectral bidirectional reflectance and effects on vegetation indices for a prairie grassland," in *Proceedings of the American Meteorological Society Symposium on FIFE*, Anaheim, Calif., Febr. 7-9, 1990, pp. 71-76.

T. F. Eck and D. W. Deering, "Spectral bidirectional hemispherical reflectance characteristics of selected sites in the Streletskaya Steppe," in *Proceedings of the International Geoscience and Remote Sensing Symposium*, Houston, Texas, May 26-29, 1992.

L. J. Fritschen, "Energy and radiation balance components for three grass surfaces near Kursk, Russia," in *Proceedings of the International Geoscience and Remote Sensing Symposium*, Houston, Texas, May 26-29, 1992.

M. Fuchs, G. Asrar, E. T. Kanemasu and L. E. Hipps, "Leaf area estimates from measurements of photosynthetically active radiation in wheat canopies," *Agricultural and Forest Meteorology*, vol. 32, pp. 13-22, 1984.

L. E. Hipps, G. Asrar and E. T. Kanemasu, "Assessing the interception of photosynthetically active radiation in winter wheat," *Agricultural Meteorology*, vol. 28, pp. 253-259, 1983.

E.B. Knipling. "Physical and physiological basis for the reflectance of visible and near-infrared radiation from vegetation," *Remote Sensing of the Environment*, vol 1, pp. 155-159, 1970.

LI-COR, Inc. LAI-2000 plant canopy analyzer: operating manual. 1991

M.A. Mesarch, E.A. Walter-Shea, B.F. Robinson, J.M. Norman and C.J. Hays. Performance evaluation and operation of a field-portable radiometer for individual leaf optical measurements. University of Neb.-Lincoln. AgMet Progress Report 91-2. 1991.

P. J. Sellers, "Canopy reflectance, photosynthesis and transpiration," *International Journal of Remote Sensing*, vol. 6, pp. 1335-1372, 1985.

P. J. Starks, *Measured and modeled radiation fluxes*. Ph.D. Dissertation, University of Nebraska, 1990, 179 pp.

P. J. Starks, J. M. Norman, B. L. Blad, E. A. Walter-Shea and C. L. Walthall, "Estimation of shortwave hemispherical reflectance (albedo) from bidirectionally reflected radiance data," *Remote Sensing Environment*, Vol. 38, pp. 123-134, 1991.

B.A. Stewart and D. R. Nielson (ed.) "Irrigation of agricultural crops." ASA, CSSA, SSSA. 1990. pp. 251-257.

R. C. Vining and B. L. Blad, "Relationship between radiometric, aerodynamic and kinetic canopy temperatures of prairie vegetation," *Proceedings of the Symposium on FIFE*, p. 106, American Meteorological Society, 1990.

E. A. Walter-Shea, B. L. Blad, C. J. Hays, M. A. Mesarch, D. W. Deering and E. M. Middleton, "Biophysical properties affecting vegetative canopy reflectance and absorbed photosynthetically active radiation at the FIFE site," *Journal of Geophysical Research-Atmosphere* (in press).

C. L. Walthall, J. M. Norman, J. M. Welles, G. Campbell and B. L. Blad, "Simple equation to approximate the bidirectional reflectance from vegetative canopies and bare soil surfaces," *Applied Optics*, Vol. 24, pp. 383-387, 1985.